IEEE Access
Multidisciplinary | Rapid Review | Open Access Journal

Received August 1, 2019, accepted August 20, 2019, date of publication August 29, 2019, date of current version September 12, 2019.

Digital Object Identifier 10.1109/ACCESS.2019.2938238

An Improved Pre-Processing Algorithm for Resolution Optimization in Galileo-Based Bistatic SAR

ZHANGFAN ZENG, ZHIMING SHI, YANLING ZHOU, YUZHANG CHEN, AND YONGCAI PAN
School of Computer Science and Information Engineering, Hubei University, Wuhan 430062, China

Corresponding author: Yanling Zhou (sunnyzhou516@126.com)

This work was supported by the National Natural Science Foundation of China (NSFC) under Grant 61601175 and Grant 61301144.

ABSTRACT Galileo based bistatic synthetic aperture radar (Galileo-BiSAR) is a subclass of passive radar, where the Galileo satellite is used as the transmitter and the receiver can be mounted on a moving vehicle or fixed on the ground. Such scheme is cost-effective and safe, and therefore can be widely used in military areas such as battle monitoring or civil scenarios such as ground deformation monitoring, change detection, etc. However, the drawback of Galileo-BiSAR system lies on the fact that, same with other passive radar, the transmitter and receiver are separately located, which introduces the necessity of pre-processing before further processing such as image formation. The existing pre-processing algorithm for Galileo-BiSAR system was established on the idea that only single band E5b signal is used. Due to its bandwidth of 20MHz, however, the range resolution of resulting image is merely up to 15m, which is not acceptable for most applications. Aimed at improving range resolution, this article proposes a new pre-processing algorithm for Galileo-BiSAR. Rather than employing the single band signal as well as duplicate of transmitting signal as the local reference signal in tradition way, a novel technique of dual matched filtering is proposed for pre-processing. Full simulations of the proposed pre-processing and further image formation were both performed. The results demonstrated the full functionality of the proposed pre-processing algorithm and verified its capability of higher resolution imaging against traditional algorithm. In addition, the paper also highlights its good computational efficiency and performance limitation against noise.

INDEX TERMS Bistatic SAR, pre-processing, resolution.

I. INTRODUCTION

Over the last decades, bistatic synthetic aperture radar (BiSAR) has seen increasing attentions from both research community and industrial area due to its extensive advantages than monostatic counterparts via the geometric separation of transmitter and receiver [1]–[9]. BiSAR system offers large varieties of configurations and topologies by employing different combinations of transmitter and receiver orientations. Among them, the GNSS based BiSAR systems (GNSS-BiSAR) are actively remarked recently [5]–[11]. In such systems, GNSS is employed as transmitter of opportunity, while the receiver can be mounted on the moving vehicle or fixed on the ground. GNSS-BiSAR system benefits from good safety, low cost, good system stability, large constellation, short revisit time and flexible configuration, etc. Generally, the transmitter can be any GNSS satellite, e.g. GPS, GLONASS, Galileo and Beidou. This paper focuses on the problem of Galileo based BiSAR, which is denoted as Galileo-BiSAR in this paper (Fig. 1).

The pre-processing is the first step for all BiSAR systems before any further processing such as image formation, in order to achieve the coherent processing [12]–[16]. The main idea of pre-processing is to extract and remove the mismatch of delay, Doppler, phase and other effects, etc. between transmitter and receiver. In this way, the subsequent processing of the pulse compression between radar channel (RC) signal and local reference signal (generated with the aid of pre-processing output) will be realized in a coherent basis. In conventional imaging BiSAR systems, either the transmitting or the receiving platform (or both) are radar platforms. One of the implications in such configurations is

The associate editor coordinating the review of this article and approving it for publication was Junjie Wu.

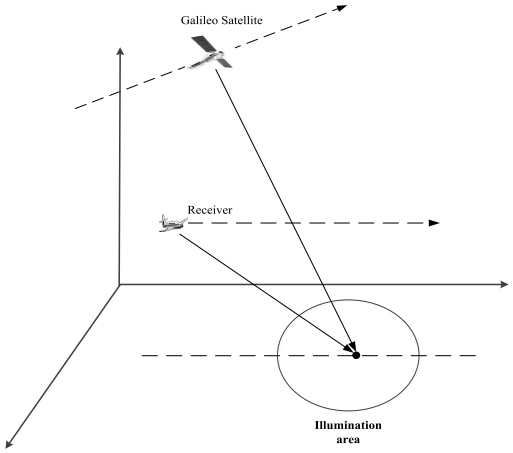

FIGURE 1. Schematic of Galileo-BiSAR.

that both the direct and reflected signal powers are significantly high. In many cases this allows a direct measurement of some parameters (e.g. delay, Doppler, phase, etc.) through techniques like signal envelope detection, or even a direct comparison between the direct and reflected signals to extract any receiver artefacts. Those pre-processing methods were well recorded in literatures [17]–[19]. Unlike conventional BiSAR system, however, GNSS-BiSAR employs the un-cooperative GNSS satellite as the transmitter. As the GNSS satellite was not originally designed for remote sensing, they lack the power budget and resolution capability of conventional imaging BiSAR [20]. As such, the approaches described above are not applicable to our case. The research work regarding GNSS-BiSAR pre-processing methods can be found in [21]–[24]. However, using only Galileo satellite single band signal E5a or E5b, the corresponding bandwidth is 20MHz and range resolution is 15m [25]. Such coarse resolution is not acceptable in most remote sensing scenarios. To address this challenge, Ma et al. proposed a spectrum combining method for Galileo-BiSAR pre-processing [26]. In their strategy, a technique called spectrum equalization was applied to a joint E5 signal, which is consisted of E5a and E5b signals. In this way, the bandwidth of the pre-processed signal can be up to 50MHz, resulting in the resolution of 6m in range direction. It is noted that, however, such algorithm is only valid in the noise-free environment and not feasible in real practice due to that spectrum equalization factor of the E5 signal can't be accurately measured in the echo signal on real time basis, whose SNR is merely −20dB even after LNA (Low Noise Amplifier) and cascade PA (Power Amplifier) [27]. To conclude, the existing pre-processing methods are insufficient in improving resolution for Galileo-BiSAR system.

This paper presents an improved pre-processing algorithm for Galileo-BiSAR system. The new algorithm proposes a novel technique of dual matched filtering to achieve optimal resolution in range direction. The rest of this paper is organized as follows. Section 2 provides the concept of Galileo-BiSAR; The traditional pre-processing was introduced in section 3; Section 4 presents the proposed pre-processing algorithm. The simulation results and discussions are described in section 5; The conclusion is drawn in section 6.

II. GALILEO-BISAR CONCEPT

Galileo-BiSAR employs Galileo satellite as the transmitter of opportunity and the receiver can be mounted on the moving platform or fixed on the ground, pointing to a certain targeting area. By coherent signal processing on the collected Galileo satellite signal reflected from this area, its objects and terrain can be reconstructed via imaging.

Galileo satellite, as the transmitter of opportunity of Galileo-BiSAR, is the European developed GNSS in last couple of decades. The main aim is to provide high precision positioning service to the Europe Zone and even all over the world for its own right. It is currently being developed by several countries within European Union (EU). Full constellation of satellites will consist of 30 vehicles. The accuracy of Galileo satellite will be better than 4m and 8m along horizontal direction and vertical direction respectively.

The Galileo satellite provides an alternative binary offset carrier (ALTBOC) based transmitted E5 signal, which could be expressed as [25]:

$$\begin{aligned} S_{E5}(t) = {} & \frac{1}{2\sqrt{2}}\left[e_{E5a-I}(t) + je_{E5a-Q}(t)\right] \\ & \times \left[\chi_{E5-s}(t) - j\chi_{E5-s}(t - T_s, E_5/4)\right] \\ & + \frac{1}{2\sqrt{2}}\left[e_{E5b-I}(t) + je_{E5b-Q}(t)\right] \\ & \times \left[\chi_{E5-s}(t) - j\chi_{E5-s}(t - T_s, E_5/4)\right] \\ & + \frac{1}{2\sqrt{2}}\left[\tilde{e}_{E5a-I}(t) + j\tilde{e}_{E5a-Q}(t)\right] \\ & \times \left[\chi_{E5-p}(t) - j\chi_{E5-p}(t - T_s, E_5/4)\right] \\ & + \frac{1}{2\sqrt{2}}\left[\tilde{e}_{E5b-I}(t) + j\tilde{e}_{E5b-Q}(t)\right] \\ & \times \left[\chi_{E5-p}(t) - j\chi_{E5-p}(t - T_s, E_5/4)\right] \end{aligned} \quad (1)$$

where T_s is the sub-carrier period, e_{E5a-I} and e_{E5b-I} are the in-phase terms of the e_{E5a} and e_{E5b} signal respectively, which contain the navigation data. e_{E5a-Q} and e_{E5b-Q} are the quadrature terms of the e_{E5a} and e_{E5b} signal respectively, which serves as the pilot signal. $\tilde{e}_{E5a-I}$, $\tilde{e}_{E5a-Q}$, $\tilde{e}_{E5b-I}$, $\tilde{e}_{E5b-Q}$ are the by-products of e_{E5a-I}, e_{E5a-Q}, e_{E5b-I} and e_{E5b-Q}. These terms are used to obtain the constant envelope of E5 signal.

Figure 2 shows the frequency spectrum of the E5 signal.

It can be observed that both E5a band and E5b band have the same bandwidth of 20.46MHz. In addition, as they are separated, it is relatively straightforward to apply either band for pre-processing and imaging, which was deeply discussed in previous work [24].

The receiver prototype of Galileo-BiSAR system is a dual channel Galileo satellite signal receiver. The heterodyne channel (HC) receives signal directly from satellite

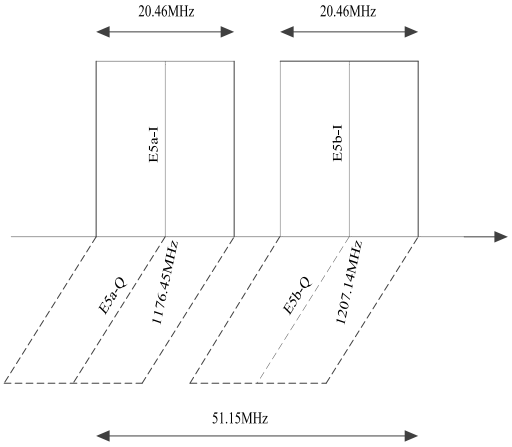

FIGURE 2. E5 signal spectrum.

for pre-processing. The radar channel records signal reflected from target area, with the purpose of image formation. The receiver constitutes a three-stage down-convertor, which transfers the received RF analog signal to the baseband digital signal. The details of the system hardware are outside the scope of this paper but can be found in [27]. The block diagram of receiver is shown in Fig. 3 for clarification.

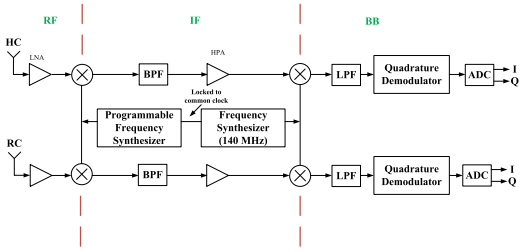

FIGURE 3. Block diagram of Galileo-BiSAR system receiver [28].

III. GALILEO-BISAR TRADITIONAL PRE-PROCESSING ALGORITHM

In this section, the traditional pre-processing algorithm for Galileo based BiSAR is briefly described. As mentioned before, the HC signal is used for pre-processing and the RC signal is used for range compression and further image formation with the aid of pre-processing output. It is also noted that the quadrature component E5a or E5b signal, i.e. e_{E5a-Q} or e_{E5b-Q} doesn't contain navigation message, which makes their pre-processing simpler. Take E5b-Q signal as an example, the HC signal and the RC signal after down-converting, demodulation and ADC could be given by [28]:

$$\begin{aligned} s_{E5b-Q,HC}(t) = & \sum_{n=1}^{T_{dwell}} e_{E5b-Q}\left[t-\tau_{E5b-Q,HC}(t)\right] \\ & \cdot c\left(t-nT_c\right) \\ & \cdot exp\left\{j\left[\begin{array}{l}2\pi f_{E5b-Q,HC}(t)\,t \\ +j\phi_{E5b-Q,HC}(t)\end{array}\right]\right\} \end{aligned} \tag{2}$$

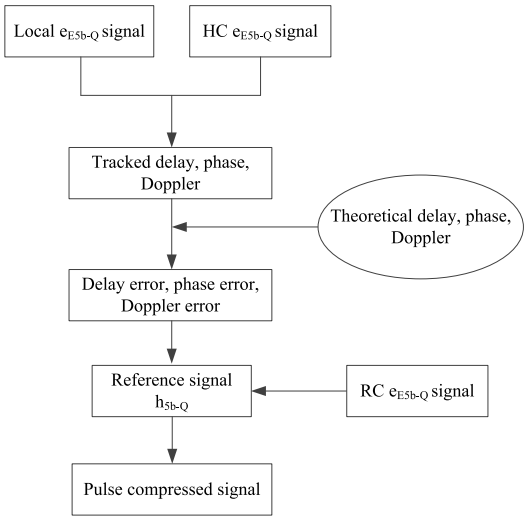

FIGURE 4. Block diagram of traditional pre-processing algorithm.

$$\begin{aligned} s_{E5b-Q,RC}(t) = & \sum_{n=1}^{T_{dwell}} e_{E5b-Q}\left[t-\tau_{E5b-Q,RC}(t)\right] \\ & \cdot c\left(t-nT_c\right) \\ & \cdot exp\left\{j\left[\begin{array}{l}2\pi f_{E5b-Q,RC}(t)\,t \\ +j\phi_{E5b-Q,RC}(t)\end{array}\right]\right\} \\ & \mathrm{n}=1,2,\ldots,T_{dwell} \end{aligned} \tag{3}$$

where T_{dwell} is the dwell time of Galileo-BiSAR.

$$\mathrm{c}(t) = \begin{cases} \dfrac{\sqrt{2}+1}{2} & t \in \left[0, \dfrac{T_c}{12}\right) \cup \left[\dfrac{7T_c}{12}, \dfrac{3T_c}{4}\right) \\ 0.5 & t \in \left[\dfrac{T_c}{12}, \dfrac{T_c}{6}\right) \cup \left[\dfrac{T_c}{2}, \dfrac{7T_c}{12}\right) \\ & \cup \left[\dfrac{3T_c}{4}, \dfrac{5T_c}{6}\right) \\ -0.5 & t \in \left[\dfrac{T_c}{6}, \dfrac{T_c}{4}\right) \cup \left[\dfrac{5T_c}{12}, \dfrac{T_c}{2}\right) \\ & \cup \left[\dfrac{5T_c}{6}, \dfrac{11T_c}{12}\right) \\ \dfrac{-\sqrt{2}+1}{2} & t \in \left[\dfrac{T_c}{4}, \dfrac{5T_c}{12}\right) \cup \left[\dfrac{11T_c}{12}, T_c\right) \end{cases} \tag{4}$$

$\tau_{E5b-Q,HC}(t)$, $f_{E5b-Q,HC}(t)$, $\phi_{E5b-Q,HC}(t)$, $\tau_{E5b-Q,RC}(t)$, $f_{E5b-Q,RC}(t)$ and $\phi_{E5b-Q,RC}(t)$ are the E5b-Q signal, delay signature, Doppler signature and phase signature of the HC signal and RC signal respectively.

The block diagram of traditional pre-processing algorithm is shown in Fig. 4 [24].

The processing steps of traditional pre-processing algorithm is described below:

- Step 1. Signal signature extraction.
  A duplicate of transmitted signal, i.e. e_{E5b-Q} is generated can be given by:

$$\mathrm{s}_0(t) = e_{E5b-Q}(t) \tag{5}$$

Then, the matched filtering of $s_{HC}(t)$ and $s_0(t)$ results in the extraction of delay, Doppler and phase of HC signal at the n^{th} chip duration, denoting As $\hat{\tau}^n_{E5b-Q,HC}$, $\hat{f}^n_{E5b-Q,HC}$ and $\hat{\phi}^n_{E5b-Q,HC}$. It is noted here that the extraction resolution is one chip duration.

- Step 2. Delay error, Doppler error and phase error estimation.
The theoretical delay history, Doppler history and phase history at the n^{th} chip duration can be obtained from the coordinates of the transmitter and receiver from third party [30], which could be given by:

$$\begin{aligned}\bar{\tau}^n_{HC} &= \frac{\left|\vec{P}_R - \vec{P}_T\right|}{c}\\ \bar{\phi}^n_{HC} &= 2\pi f_c \bar{\tau}^n\\ \bar{f}^n_{HC} &= d\bar{\phi}^n_{HC}\end{aligned} \tag{6}$$

where $\vec{P}_R$ and $\vec{P}_T$ represents the coordinates of receiver and transmitter respectively. $|\cdot|$ defines the determine of a matrix. c is the speed of light wave, f_c is the operational frequency of Galileo satellite.$d$defines the differential operation.
Then, the delay error, Doppler error and phase error of the HC signal will be given by:

$$\begin{aligned}\Delta\tau^n_{E5b-Q,HC} &= \hat{\tau}^n_{E5b-Q,HC} - \bar{\tau}^n_{HC}\\ \Delta\phi^n_{E5b-Q,HC} &= \hat{\phi}^n_{E5b-Q,HC} - \bar{\phi}^n_{HC}\\ \Delta f^n_{E5b-Q,HC} &= \hat{f}^n_{E5b-Q,HC} - \bar{f}^n_{HC}\end{aligned} \tag{7}$$

It is noted that, as those errors are introduced by the effects such as atmosphere effects, thermo-noise, etc. They are identical in radar channel as well. The mathematical expressions of delay error, Doppler error and phase error of the RC signal can be given by:

$$\begin{aligned}\Delta\tau^n_{E5b-Q,RC} &\simeq \Delta\tau^n_{E5b-Q,HC}\\ \Delta\phi^n_{E5b-Q,RC} &\simeq \Delta\phi^n_{E5b-Q,HC}\\ \Delta f^n_{E5b-Q,RC} &\simeq \Delta f^n_{E5b-Q,HC}\end{aligned} \tag{8}$$

- Step3. Reference signal generation.
The reference signal for following pulse compression could be generated as:

$$\begin{aligned}&h_{E5b-Q}(t)\\ &= \sum_{n=1}^{T_{dwell}} e_{E5b-Q}\left[t - \Delta\tau^n_{E5b-Q,RC}\right]\\ &\quad \times \mathrm{c}\left(t - nT_c\right)\exp\left\{j\left[\begin{matrix}2\pi\,\Delta f^n_{E5b-Q,RC}t\\ +\Delta\phi^n_{E5b-Q,RC}\end{matrix}\right]\right\}\end{aligned} \tag{9}$$

- Step 4. Pulse compression between reference signal and RC signal.
The pulse compressed signal can be given by:

$$\begin{aligned}&PC_{E5b-Q}(\tau)\\ &= MF\left[h_{E5b-Q}(t), s_{E5b-Q,RC}(t)\right]\\ &= \sum_{t=0}^{T_c} s_{E5b-Q,RC}(\tau - t)\cdot h^1_{E5b-Q}(t)\\ &= \sum_{n=1}^{T_{dwell}} R_{E5b-Q}\left[\tau - \tilde{\tau}^n_{E5b-Q}\right]\\ &\quad \cdot \exp\left\{j\left[\begin{matrix}2\pi\tilde{f}^n_{E5b-Q}\tau\\ +\tilde{\phi}^n_{E5b-Q}\end{matrix}\right]\right\}\end{aligned} \tag{10}$$

where $MF[\cdot]$ defines the mathematical operation of matched filtering. $R_{E5b-Q}[\cdot]$ defines the triangular shaped envelope of the matched filtered function between reference signal and RC signal. τ is the delay shift in the matched filtering operation. $\tilde{\tau}^n_{E5b-Q}$, $\tilde{\phi}^n_{E5b-Q}$ and $\tilde{f}^n_{E5b-Q}$ are the compensated delay, Doppler and phase signatures of pulse compressed signal at the n^{th} chip duration, which are written as:

$$\begin{aligned}\tilde{\tau}^n_{E5b-Q} &= \tau^n_{E5b-Q,RC} - \Delta\tau^n_{E5b-Q,RC}\\ \tilde{\phi}^n_{E5b-Q} &= \phi^n_{E5b-Q,RC} - \Delta\phi^n_{E5b-Q,RC}\\ \tilde{f}^n_{E5b-Q} &= f^n_{E5b-Q,RC} - \Delta f^n_{E5b-Q,RC}\end{aligned} \tag{11}$$

It can be observed from Eq. (11) that after error removal, these three parameters are only formed by the signal propagation [24].

As the pulse compressed signal, i.e. $PC_{E5b-Q}(t)$ has the same nature with auto-correlation function of E5b-Q signal, especially in terms of resolution, the brief simulation of E5b-Q auto-correlation is sufficient here. The comprehensive simulation result of pre-processing will be in shown in section 5. Fig. 5 presents the auto-correlation function of E5b-Q signal.

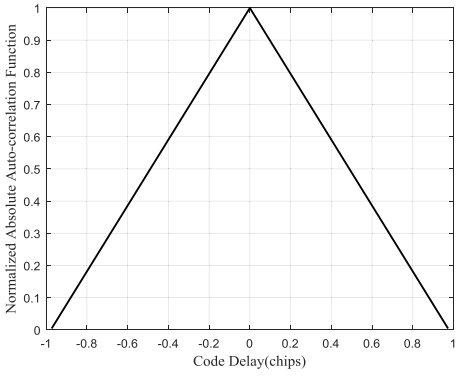

FIGURE 5. Auto-correlation function of E5b-Q signal.

It can be found from Fig. 5 that the impulse response width of the compressed signal occupies the while chip duration, which conforms to the theoretical expectation. In addition, the range resolution of Galileo-BiSAR could be obtained from the value of the impulse response width at 0.707, which is attributed only to the bandwidth of the radar signal

To improve the resolution, however, the most straightforward way to mind is to narrow the impulse response width of the cross-correlation function, which in turn, to increase

the bandwidth on its own. To this end, a joint band E5-Q signal, consisting of E5a-Q signal and E5b-Q signal, with the bandwidth of 50MHz is employed. The pulse compression result of direct adoption of the traditional pre-processing algorithm to the E5-Q signal can be written as:

$$\begin{aligned} PC_{E5-Q}(\tau) &= MF\left[h_{E5-Q}(t), s_{E5-Q,RC}(t)\right] \\ &= \sum_{t=0}^{T_c} s_{E5-Q,RC}(\tau - t)\cdot h^1_{E5-Q}(t) \\ &= \sum_{n=1}^{T_{dwell}} R_{E5-Q}\left[\tau - \tilde{\tau}^n_{E5-Q}\right] \\ &\quad \cdot exp\left\{j\left[\begin{matrix}2\pi\tilde{f}^n_{E5-Q}\tau \\ +\tilde{\phi}^n_{E5-Q}\end{matrix}\right]\right\} \end{aligned} \tag{12}$$

where $R_{E5-Q}[\cdot]$ defines the auto-correlation envelope of the matched filtered function between reference signal and E5-Q joint band RC signal. $\tilde{\tau}^n_{E5-Q}$, $\tilde{\phi}^n_{E5-Q}$ and $\tilde{f}^n_{E5-Q}$ are the compensated delay, Doppler and phase signatures of pulse compressed E5-Q joint band signal, which are introduced only from signal propagation

Same as mentioned before, the simulation result of auto-correlation function of E5-Q signal is shown in Fig. 6.

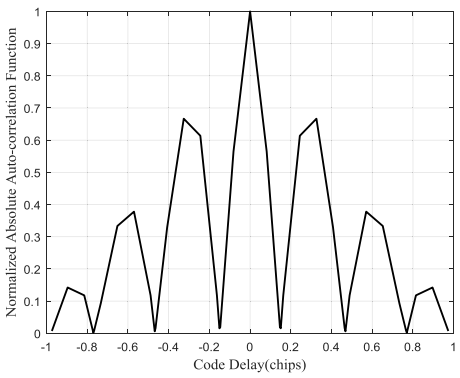

FIGURE 6. Auto-correlation function of E5-Q signal.

It can be observed that the joint band E5-Q signal is well focused and the width of the main-lobe is one third of that of single band E5b-Q signal as shown in Fig. 5, which would imply three times better resolution. It is noted that, however, the magnitudes of the first side-lobe is only -3.5dB lower than the main lobe, which would introduce false alarms in the imaging. Therefore, joint band signal with traditional pre-processing algorithm is not suitable for imagery application.

IV. GALILEO-BISAR PROPSED PRE-PROCESSING ALGORITHM

In this section, a novel pre-processing algorithm is proposed to realize the optimal impulse response width and keep the side-lobes minimum in Fig. 6. The new algorithm employs a specially designed technique of dual matched filtering. The block diagram of the new algorithm is shown in Fig. 7:

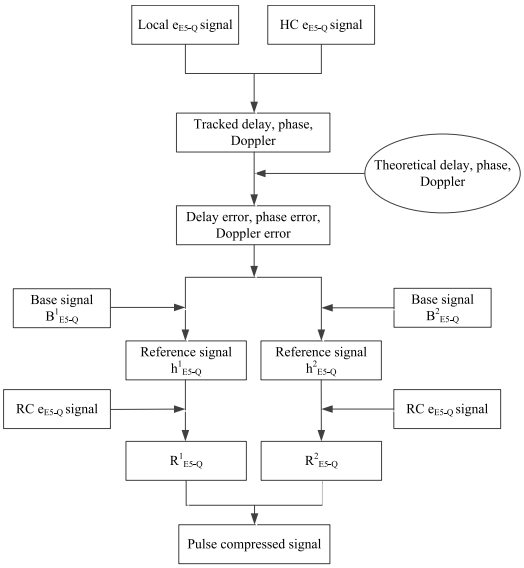

FIGURE 7. Block diagram of the proposed pre-processing algorithm.

The processing steps of the proposed algorithm is described as follows:

- Step 1. Same with the step 1 and 2 in traditional algorithm, the ultimate delay error, Doppler error and phase error at the n^{th} chip duration are obtained and are given as:

$$\begin{aligned} \Delta\tau^n_{E5-Q,HC} &= \hat{\tau}^n_{E5-Q,HC} - \bar{\tau}^n_{HC} \\ \Delta\phi^n_{E5-Q,HC} &= \hat{\phi}^n_{E5-Q,HC} - \bar{\phi}^n_{HC} \\ \Delta f^n_{E5-Q,HC} &= \hat{f}^n_{E5-Q,HC} - \bar{f}^n_{HC} \end{aligned} \tag{13}$$

where $\hat{\tau}^n_{E5-Q,HC}$, $\hat{f}^n_{E5-Q,HC}$ and $\hat{\phi}^n_{E5-Q,HC}$ are the extracted delay history, Doppler history and phase history of the E5-Q joint band HC signal at the n^{th} chip duration. Alike Eq. (7), the counterparts of E5-Q joint band RC signal can be given by:

$$\begin{aligned} \Delta\tau^n_{E5-Q,RC} &\simeq \Delta\tau^n_{E5-Q,HC} \\ \Delta\phi^n_{E5-Q,RC} &\simeq \Delta\phi^n_{E5-Q,HC} \\ \Delta f^n_{E5-Q,RC} &\simeq \Delta f^n_{E5-Q,HC} \end{aligned} \tag{14}$$

- Step 2. Reference signal generation, the details are described as follows:
  First, two base signals are defined as:

$$B^1_{E5-Q}(t) = \begin{cases} \sqrt{12} & t \in \left(0, \dfrac{T_c}{12}\right] \\ 0 & t \in \left(\dfrac{T_c}{12}, T_c\right) \end{cases} \tag{15}$$

$$B^2_{E5-Q}(t) = B^1_{E5-Q}(T_c - t) \tag{16}$$

The waveforms of $B^1_{E5-Q}(t)$ and $B^2_{E5-Q}(t)$ are shown in Fig. 8:

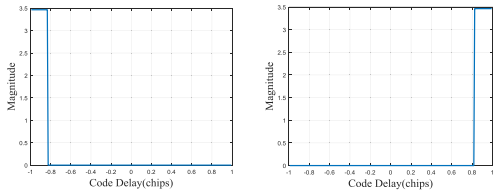

FIGURE 8. Waveforms of B^1_{E5-Q} and $B^2_{E5-Q}(t)$.

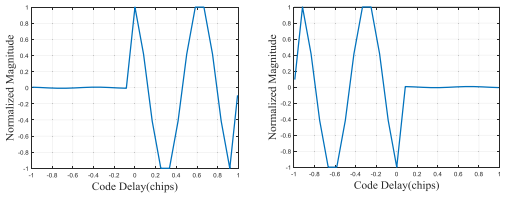

FIGURE 9. Waveforms of $R^1_{E5-Q}(\tau)$ and $R^2_{E5-Q}(\tau)$.

Then, based on Eq. (14), Eq. (15) and Eq. (16), two reference signal can be given by:

$$h^1_{E5-Q,1}(t) = \sum_{n=1}^{T_{dwell}} B_1\left[\mathrm{t} - \Delta\tau^n_{E5-Q,RC}\right] \cdot c\left(t - nT_c\right) \cdot \exp\left\{j\left[\begin{array}{c}2\pi\,\Delta f^n_{E5-Q,RC}t \\ +\Delta\phi^n_{E5-Q,RC}\end{array}\right]\right\} \quad (17)$$

$$h^2_{E5-Q}(t) = \sum_{n=1}^{T_{dwell}} B_2\left[t - \Delta\tau^n_{E5-Q,RC}\right] \cdot c\left(t - nT_c\right) \cdot \exp\left\{j\left[\begin{array}{c}2\pi\,\Delta f^n_{E5-Q,RC}t \\ +\Delta\phi^n_{E5-Q,RC}\end{array}\right]\right\} \quad (18)$$

- Step 3. Pulse integration between reference signal and RC signal via the application of proposed technique of dual matched filtering, the details are given as follows: The matched filtering between received joint band signal $s_{E5-Q,RC}(t,u)$ and two local base signals are given as:

$$\begin{aligned} R^1_{E5-Q}(\tau) &= MF\left[h^1_{E5-Q}(t), s_{E5-Q,RC}(t)\right] \\ &= \sum_{t=0}^{T_c} s_{E5-Q,RC}(\tau - t)\cdot h^1_{E5-Q}(t) \\ &= \sum_{n=1}^{T_{dwell}} R_{b1,E5-Q}\left[\tau - \tilde{\tau}^n_{E5-Q}\right] \cdot exp\left\{j\left[\begin{array}{c}2\pi\tilde{f}^n_{E5-Q}\tau \\ +\tilde{\phi}^n_{E5-Q}\end{array}\right]\right\} \end{aligned} \quad (19)$$

$$\begin{aligned} R^2_{E5-Q}(\tau) &= MF\left[h^2_{E5-Q}(t), s_{E5-Q,RC}(t)\right] \\ &= \sum_{t=0}^{T_c} s_{E5-Q,RC}(\tau - t)\cdot h^2_{E5-Q}(t) \\ &= \sum_{n=1}^{T_{dwell}} R_{b2,E5-Q}\left[\tau - \tilde{\tau}^n_{E5-Q}\right] \cdot exp\left\{j\left[\begin{array}{c}2\pi\tilde{f}^n_{E5-Q}\tau \\ +\tilde{\phi}^n_{E5-Q}\end{array}\right]\right\} \end{aligned} \quad (20)$$

where $R^1_{E5-Q}(\tau)$, $R^2_{E5-Q}(\tau)$ represent the two matched filtering results, which are shown in Fig. 9

The pulse integration is performed via following equation:

$$PC_{E5-Q}(\tau) = \left|R^1_{E5-Q}(\tau)\right| + \left|R^2_{E5-Q}(\tau)\right| - \left|R^1_{E5-Q}(\tau) + R^2_{E5-Q}(\tau)\right| \quad (21)$$

where $|\cdot|$ defines the operation of modulo.

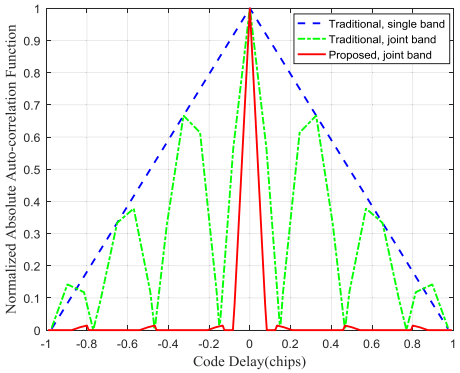

FIGURE 10. Pulse compression results comparison.

The pulse integration result of the joint band E5-Q signal in one chip duration by proposed algorithm is shown in Fig. 10. In this figure, the latest result shown in red solid line is overlapped with the results of single band E5b-Q signal (Fig. 6) and joint band E5-Q signal (Fig. 7) by traditional algorithm, which are shown in blue dashed line and green dotted line respectively for comparison.

It is apparent from Fig. 10 that the proposed algorithm removes all the side-lobes and results in a better resolution by more than three times as well as less false alarm (i.e. less side-lobes) than the others to a large extent.

V. SIMULATION AND DISCUSSION

A. POINT SPREAD FUNCTION SIMULATION AND ANALYSIS

Simulation experiments were made to verify the performance of the proposed pre-processing algorithm for Galileo-BiSAR system. For the sake of comparison, the simulations were implemented for three scenarios:

1) Single band E5b-Q signal with traditional pre-processing algorithm.
2) Joint band E5-Q signal with traditional pre-processing algorithm.
3) Joint band E5-Q signal with proposed pre-processing algorithm.

It is noted that, the simulation results of pre-processing is not visible as the pulse compressed RC signal is buried in the noise. However, those can be checked once the images are formed. As a result, an integrated simulations including pre-processing and imaging are performed in this section. At the current stage, PSF (Point Spread Function) is sufficient

to verify the proposed technique. In addition, for the sake of accuracy, Back-Projection Algorithm (BPA) is employed to focus the pre-processed data.

Table 1 presents the simulation parameters, which are similar to the real experiments to a large extent as in [30]. GIOVE-A is used as the transmitter. The dwell time is 100 seconds. The satellite trajectory is obtained from the GNSS open sources [29]. It is significantly noted that the noise is added to RC signal to emulate the SNR of −20dB [27].

The simulated images of the three scenarios are shown in Fig. 11 (a), Fig. 11 (c) and Fig. 11 (e) respectively, while the corresponding cross-sections of the range direction are shown in Fig. 11 (b), Fig.11 (d) and Fig.11 (f) respectively.

TABLE 1. Simulation parameters.

Parameter	Value
Transmitter	GIOVE-A
Carrier frequency	1191.795 MHz
Chip rate	10.23 MHz
Sampling rate	50 MHz
Pulse Repeat Frequency	1000 Hz
Dwell time	100 sec
SNR	-20dB

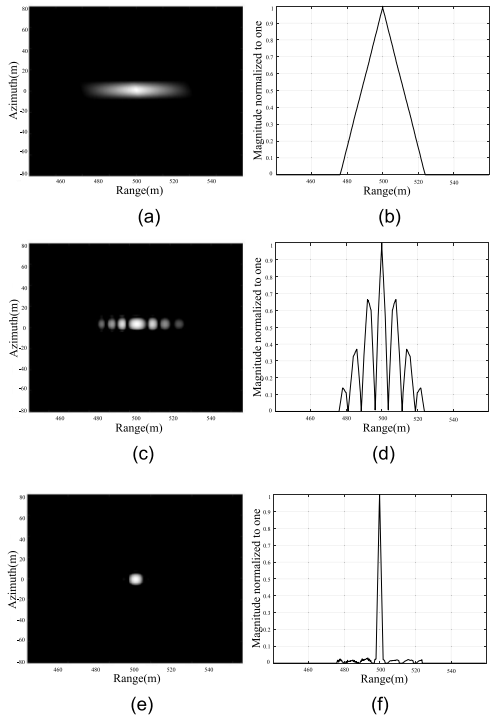

FIGURE 11. Imaging result and range cross-section (a) Single band E5b-Q signal imaging, (b) Range cross-section of Fig. 9(a), (c) Joint band E5-Q signal imaging with traditional pre-processing algorithm, (d) Range cross-section of Fig. 9(c), (e) Joint band E5-Q signal imaging with proposed pre-processing algorithm, (f) Range cross-section of Fig. 9(e).

It could be found from Fig. 11 that the range resolution is improved from 15m to 4m after employing proposed pre-processing algorithm to the joint band E5-Q signal, given the same image formation algorithm, i.e. BPA applied. In addition, the cross-sections of the images at range directions are in good coincidence with the simulated ones as shown in Fig. 10.

B. COMPUTATIONAL EFFICIENCY

The computational complexity of the proposed pre-processing algorithm was considered in this section. The comparison was made between proposed algorithm and traditional counterpart [24].

Let a single chip signal consists of N_t samples and the dwell time consists of N_u chips. Let the running time of a single operation of addition, subtraction, and multiplication is T_{add}, T_{sub} and T_{mul} respectively, According to Eq. (2) to Eq. (21), the operations required by the traditional algorithm [24] and the proposed algorithm could be expressed as:

$$\begin{aligned} N_{old} &= (3N_t logN_t + 2N_t)N_u T_{mul} \\ &\quad + 6N_t logN_t N_u T_{add} + N_t N_u T_{sub} \end{aligned} \tag{22}$$

$$\begin{aligned} N_{new} &= (4.5N_t logN_t + 3N_t)N_u T_{mul} \\ &\quad + (9N_t logN_t + 3N_t)N_u T_{add} + N_t N_u T_{sub} \end{aligned} \tag{23}$$

The operational time difference of proposed algorithm against conventional algorithm can be given by:

$$\begin{aligned} N_{diff} &= N_{new} - N_{old} \\ &= (1.5N_t logN_t + N_t)N_u T_{mul} \\ &\quad + (3N_t logN_t + 3N_t)N_u T_{add} \end{aligned} \tag{24}$$

A typical scenario with Galileo-BiSAR is given by these parameters:

$$\begin{aligned} N_t &= 50000 \\ N_u &= 100000 \\ T_{add} &= 1/10000000000 \\ T_{mul} &= 1/1000000000 \end{aligned}$$

Then the operational delay of proposed algorithm against traditional algorithm is merely less than 1 minute, which is acceptable in most off-line scenarios.

C. PERFORMANCE LIMITATION

This section provides a general discussion of the performance limitation of the proposed pre-processing algorithm against noise level from both theoretical and simulation level. It should be noted that, however, as the performance of the target recognition can only be evaluated at the stage of imaging, the joint performance limitation including both pre-processing algorithm and azimuth compression algorithm leading to the final image is discussed in this section. Generally, the joint performance depends on the total pulse compression power gain in the full lifecycle of image formation. The total pulse compression gain is consisted of pulse compression gain at range direction and azimuth direction, which is highly related to the trial parameters such as bistatic

TABLE 2. Simulation parameters.

Parameter	Value
G_r(dB)	40dB
B_a	200 Hz
Dwell time(T_{dwell})	100 sec

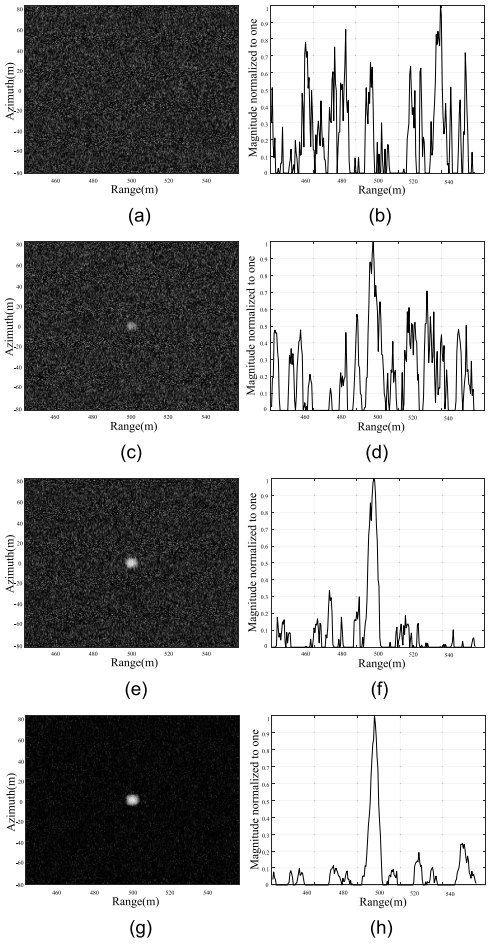

FIGURE 12. Imaging result and range cross-section (a, b) −126dB, (c, d) −120dB, (e, f) −114dB, (g, h) −108dB.

topology, chip duration, signal structure, dwell time, pulse repetition frequency, etc. The analytical formula of pulse compression power gain can be given by:

$$\begin{aligned} G_{total}(\text{dB}) &= G_r(\text{dB}) + G_a(\text{dB}) \\ &= G_r(\text{dB}) + 20log_{10}(B_a \times T_{dwell}) \end{aligned} \quad (25)$$

where G_r(dB) is the pulse compression power gain at range direction, which can be calculated at given chip duration and sampling rate. B_a is the generated azimuth bandwidth duration the dwell time and T_{dwell} is the dwell time. B_a can be calculated at given bistatic topology and dwell time.

With the same simulation parameters in Table 1, the values of the three parameters mentioned above have been calculated and are listed in the Table 2:

Then applying Eq. (25), the total pulse compression power gain i.e. G_{total}(dB) will be 126dB. In other words, the target will not be visible if the signal-to-noise ratio is lower than −126dB in this specific simulation scenario. To better explain what will happen in severe noisy environment, a set of imaging simulations at different SNR levels: −126dB, −120dB, −114dB and −108dB is performed and the results are shown in Fig. 12. The finally formed images after using proposed pre-processing algorithm and Back-projection imaging algorithm (Back-projection imaging algorithm is performed in the time domain, it is more accuracy than any frequency domain algorithms and it is usually used for prototype verification and calibration) are shown in Fig. 12 (a), (c), (e) and (g), while their corresponding range cross-sections of the zero azimuth distance are shown in Fig. 12(b), (d), (f) and (h).

It can be found from the above results that with the growing SNR, the point target becomes gradually visible. In addition, at SNR = −126dB, the target can't be seen, which conforms to the theoretical expectation. It should be noted that, however, the discussion described above is the theoretical evaluation in ideal scenario. In real practice, due to various hardware impacts, imaging impacts and speckle noise introduced duration SAR imaging, the SNR should be higher to maintain the acceptable performance.

VI. CONCLUSION

This paper presents a novel pre-processing algorithm for Galileo-BiSAR system, with the aim of resolution improvement. The proposal is achieved by applying a specially designed technique of dual matched filtering on the joint band of E5-Q signal rather than single E5a-Q/E5b-Q signal of traditional way. Current simulation results show that all the side-lobes have been removed and the resolution in the range direction can be improved more than three times via proposed algorithm as well as less false alarms. In addition, the computational complexity of the proposal is discussed against the traditional algorithm. Calculation indicates that the proposed algorithm is achieved at the expense of some operational delay, which is, however, acceptable in most off-line scenarios. What is more, the analysis of the performance limitation indicates that the proposed pre-processing algorithm validates if the SNR of the received signal is higher than −126dB from theoretical perspective. It is concluded that the proposed algorithm allows a better resolution in great length at a little expense of computational complexity. It is also noted that, due to the signal of Beidou satellite from China has high level of similarity with Galileo signal, the proposed pre-processing algorithm may be applicable to Beidou based radar system as well.

The next step of work will divert to the investigation of pre-processing algorithm of other type of GNSS-BiSAR system.

ACKNOWLEDGMENT

The authors thank Prof. Feifeng Liu from Beijing Institute of Technology, Prof. Qilei Zhang from National Defense

University of Technology for their on-going interest and support of this work.

REFERENCES

[1] T. Espeter, I. Walterscheid, J. Klare, A. R. Brenner, and J. H. G. Ender, "Bistatic forward-looking SAR: Results of a spaceborne-airborne experiment," *IEEE Geosci. Remote Sens. Lett.*, vol. 8, no. 4, pp. 765–768, Mar. 2011.

[2] X. Qiu, D. Hu, and C. Ding, "Some reflections on bistatic SAR of forward-looking configuration," *IEEE Geosci. Remote Sens. Lett.*, vol. 5, no. 4, pp. 735–739, Oct. 2008.

[3] W. Li, Y. Yang, J. Huang, J. Kong, and L. Wu, "An improved radon-transform-based scheme of Doppler centroid estimation for bistatic forward-looking SAR," *IEEE Geosci. Remote Sens. Lett.*, vol. 8, no. 2, pp. 379–383, Mar. 2011.

[4] Z. Shi, Z. Zeng, Y. Zhou. W. Liu, Y. Pan, and T. Lan, "Point spread function generation method of geo-stationary GNSS based bistatic forward looking SAR," *Optik*, vol. 179, pp. 189–194, Feb. 2019.

[5] T. Espeter, I. Walterscheid, J. Klare, A. R. Brenner, and J. H. G. Ender, "Bistatic forward-looking SAR: Results of a spaceborne–airborne experiment," *IEEE Geosci. Remote Sens. Lett.*, vol. 8, no. 4, pp. 765–768, Jul. 2011.

[6] H.-S. Shin and G.-T. Lim, "Omega-k algorithm for airborne forward-looking bistatic spotlight SAR imaging," *IEEE Geosci. Remote Sens. Lett.*, vol. 6, no. 2, pp. 765–768, Apr. 2011.

[7] J. Wu, Z. Li, Y. Huang, J. Yang, H. Yang, and Q. H. Liu, "Focusing bistatic forward-looking SAR with stationary transmitter based on keystone transform and nonlinear chirp scaling," *IEEE Geosci. Remote Sens. Lett.*, vol. 11, no. 1, pp. 148–152, Jan. 2014.

[8] M. Antoniou, M. Cherniakov, and C. Hu, "Space-surface bistatic SAR image formation algorithms," *IEEE Trans. Geosci. Remote Sens.*, vol. 47, no. 6, pp. 1827–1843, Jun. 2009.

[9] C. Hu, T. Long, Z. Liu, T. Zeng, and Y. Tian, "An improved frequency domain focusing method in geosynchronous SAR," *IEEE Trans. Geosci. Remote Sens.*, vol. 52, no. 9, pp. 5514–5528, Sep. 2014.

[10] T. Zeng, M. Cherniakov, and T. Long, "Generalized approach to resolution analysis in BSAR," *IEEE Trans. Aerosp. Electron. Syst.*, vol. 41, no. 2, pp. 461–474, Apr. 2005.

[11] M. Antoniou, Z. Zeng, L. Feifeng, and M. Cherniakov, "Experimental demonstration of passive BSAR imaging using navigation satellites and a fixed receiver," *IEEE Geosci. Remote Sens. Lett.*, vol. 9, no. 3, pp. 477–481, May 2012.

[12] W. Tian, H. Liu, and T. Zeng, "Frequency and time synchronization error analysis based on generalized signal model for bistatic SAR," in *Proc. IET Int. Radar Conf.*, Apr. 2009, pp. 1–4.

[13] W. Tian, S. Hu, and T. Zeng, "A frequency synchronization scheme based on PLL for BiSAR and experiment result," in *Proc. Int. Conf. Signal Process. (ICSP)*, Oct. 2008, pp. 2425–2428.

[14] W. Wang, "GPS-based time & phase synchronization processing for distributed SAR," *IEEE Trans. Aerosp. Electron. Syst.*, vol. 45, no. 3, pp. 1040–1051, Jul. 2009.

[15] W.-Q. Wang, "Design of frequency synthesizer for synchronizing airborne bistatic SAR systems," in *Proc. IEEE Aerosp. Conf.*, Mar. 2008, pp. 1–10.

[16] W.-Q. Wang, Q. Peng, and J. Cai, "Phase synchronization errors on near-space passive bistatic radar imaging," in *Proc. IEEE Circuits Syst. Int. Conf. Test. Diagnosis*, Apr. 2009, pp. 1–4.

[17] P. Lopez-Dekker, J. J. Mallorgui, P. Serra-Morales, and J. Sanz-Marcos, "Phase synchronization and Doppler centroid estimation in fixed receiver bistatic SAR systems," *IEEE Trans. Geosci. Remote Sens.*, vol. 46, no. 11, pp. 3459–3471, Nov. 2008.

[18] Z. He, F. He, J. Chen, H. Huang, Z. Dong, and D. Liang, "Echo-domain phase synchronization algorithm for bistatic SAR in alternating bistatic/Ping–Pong mode," *IEEE Geosci. Remote Sens. Lett.*, vol. 9, no. 4, pp. 604–608, Jul. 2012.

[19] W. Wang "Approach of adaptive synchronization for bistatic SAR real-time imaging," *IEEE Trans. Geosci. Remote Sens.*, vol. 45, no. 9, pp. 2695–2700, Sep. 2007.

[20] J. Tsui, *Digital Techniques for Wideband Receivers*. Norwood, MA, USA: Artech House, 1995.

[21] R. Saini, R. Zuo, and M. Cherniakov, "Signal sychronisation in SS-BSAR based on GLONASS satellite emission," in *Proc. IET Int. Conf. Radar Syst.*, Oct. 2007, pp. 1–5.

[22] R. Saini, R. Zuo, and M. Cherniakov, "Problem of signal synchronisation in space-surface bistatic synthetic aperture radar based on global navigation satellite emissions—Experimental results," *IET Radar, Sonar Navigat.*, vol. 4, no. 1, pp. 110–125, Feb. 2010.

[23] H. Zhou, M. Antoniou, Z. Zeng, R. Zuo, H. Tan, J. Guo, and M. Cherniakov, "Pre-processing for time domain image formation in SS-BSAR system," *J. Syst. Eng. Electron.*, vol. 23, no. 6, pp. 875–880, Dec. 2012.

[24] Z. Zeng, "Generic signal synchronisation algorithm for passive global navigation satellite system-based synthetic aperture radar," *IET Radar Sonar Navigat.*, vol. 9, no. 4, pp. 364–373, Apr. 2015.

[25] *Signal in Space Interface Control Document*, document, European GNSS Service Center, Prague, Czech Republic, 2010.

[26] H. Ma, M. Antoniou, and M. Cherniakov, "Passive GNSS-based SAR resolution improvement using joint Galileo E5 signals," *IEEE Geosci. Remote Sens. Lett.*, vol. 12, no. 8, pp. 1640–1644, Aug. 2015.

[27] Z. Zeng, "Passive bistatic SAR with GNSS transmitter and a stationary receiver," Ph.D. dissertation, School Electron., Elect. Comput. Eng., Univ. Birmingham, Birmingham, U.K., 2013.

[28] J. Ren, W. Jia, H. Chen, and M. Yao, "Unambiguous tracking method for alternative binary offset carrier modulated signals based on dual estimate loop," *IEEE Commun. Lett.*, vol. 16, no. 11, pp. 1737–1740, Nov. 2012.

[29] *IGS Website*. [Online]. Available: http://www.igs.org

[30] M. Antoniou, Z. Hong, Z. Zhangfan, R. Zuo, sQ. Zhang, and M. Cherniakov, "Passive bistatic synthetic aperture radar imaging with Galileo transmitters and a moving receiver: Experimental demonstration," *IET Radar, Sonar Navigat.*, vol. 7, no. 9, pp. 985–993, Dec. 2013.

ZHANGFAN ZENG received the B.S. degree from Wuhan University, China, in 2006, the M.S. degree from The University of Manchester, U.K., in 2007, and the Ph.D. degree from the University of Birmingham, U.K., in 2013, all in communication engineering. From 2008 to 2009, he was an Algorithm Engineer with Guangdong Nortel Network, China. From 2013 to 2014, he was a Protocol Stack Software Engineer with NextG-Com Ltd., Staines-upon-Thames, U.K. From January 2015 to September 2015, he was a Senior Engineer with Cobham Wireless, Stevenage, U.K. Since December 2015, he has been a full-time Associate Professor with Hubei University, China. He has published over 20 research articles. He holds one patent in radar community. His research interests include wireless communication and digital signal processing.

ZHIMING SHI received the bachelor's degree from Zhixing College, Hubei University, where he is currently pursuing the master's degree. He is focusing on passive radar signal processing. He has published four articles in this area.

YANLING ZHOU received the B.Sc., M.Sc., and Ph.D. degrees from the Huangzhong University of Science and Technology, China. She is currently a full time Associate Professor with Hubei University. She is an expert in navigation satellite signal receiving techniques and has published 10 leading papers in this field.

YUZHANG CHEN received the B.S., M.S., and Ph.D. degrees from the Huazhong University of Science and Technology, China. He is currently a full-time Associate Professor with Hubei University. He is focusing on image processing. He has published 20 articles in this area.

YONGCAI PAN is currently a Full Professor and the Head of the Laboratory of Signal Processing and System Analysis, Hubei University. His research interests include wireless communication, signal processing, and intelligent systems.